Investigation of torsional teeth stiffness and second moment of area calculations for an analytical model of spline coupling behaviour

A Barrot, Marc Sartor, Manuel Paredes

Investigation of torsional teeth stiffness and second moment of area calculations for an analytical model of spline coupling behaviour

A. Barrot, M. Sartor, M. Paredes

INSA de Toulouse, LGMT, 137 Av. de Rangueil, 31077 Toulouse Cedex, France

Abstract

Torque distribution from within spline coupling is an important matter for design engineers wishing to study the behaviour of spline couplings. This distribution can be estimated thanks to an analytical equation, based on material, torsional teeth stiffness, and second moments of area of the shaft and sleeve. These parameters have to be determined precisely. The material properties can be readily determined but calculation of the other parameters requires finite element calculations or complex algorithms. The aim is to propose simplified equations so as rapidly to obtain values for both teeth stiffness and second moments of area. Experimental designs were implemented to determine the most appropriate equations. Torsional stiffness is the first parameter studied in the present paper. This is the result of rotations due to various phenomena involving distortions such as bending, shear, compression, rotation of the foundation of the teeth and the teeth sliding. Two simplified equations are finally expressed to define torsional stiffness. The first takes into account the four first phenomena and the second one the teeth sliding. The second topic in the present paper covers the influence on torque distribution of various formulae for calculating second moments of area. A solution, which takes into account shear of the teeth, is highlighted.

Keywords: spline coupling, teeth stiffness, second moment of area, experimental design

Notations

α	Tilted angle in radians
β_0	Corrective coefficient for the second moment of area of the shaft which minimizes the gap between analytical and FE torque distribution
β	Corrective coefficient for the second moment of area of the shaft
θ_b	Rotation due to bending of the sleeve and shaft in radians
θ_c	Rotation due to compression of the sleeve and shaft in radians
θ_f	Rotation due to the foundation rotation of the sleeve and shaft in radians
θ_g	Sum of all rotations: θ_{ws}, θ_{sl} in radians
θ_s	Rotation due to shear of the sleeve and shaft in radians
θ_{sl}	Rotation due to sliding of the sleeve and shaft in radians
θ_{ws}	Sum of four rotations: θ_b, θ_s, θ_f, θ_c in radians
φ^j, φ^e	Twisting angles for the internal spline and external spline in radians
ϕ	Contact angle at the pitch radius in radians
ϕ_p	Contact load angularity at the pitch radius in radians
c_φ	Torsional teeth stiffness per unit width in N/rad
D	Pitch diameter in metres
D_{ext}, R_{ext}	External diameter and radius of the sleeve in metres
D_o, D_i	Shaft and sleeve major diameter in metres
D_{int}, R_{int}	Diameter and radius corresponding to the hole of the shaft in metres
D_{re}, R_{re}	Diameter and radius of the teeth foundation of the shaft in metres
D_{ri}, R_{ri}	Diameter and radius of the teeth foundation of the sleeve in metres
E^e, E^i	Young's modulus of internal spline and external splines in Pa
E_0	Average of responses
E_1, E_2 E_3	Effects respectively of factors m, N and m N interaction

F	Force applied on the contact surface per unit width in N/m
G^i, G^e	Shear modulus of the internal and external spline in Pa
I^e, I^i	Shaft and sleeve tooth second moment of area in m^4
I^e_p, I^i_p	Second moments of area of the shaft and sleeve calculated with the pitch diameter in m^4
I^e_s, I^i_s	Second moments of area of the shaft and sleeve calculated with the influence of the teeth shear in m^4
I^e_t, I^i_t	Second moments of area of the shaft and sleeve calculated with the teeth extremities diameters in m^4
k_F	Corrective coefficient, optimising rotation due to sliding
L	Spline coupling length in metres
m	Modulus in metres
N	Number of teeth
P	Circular pitch in metres
R	Pitch radius in metres
$R_{0,}$ R_i	Shaft and sleeve major radius in metres
R_b	Base radius of the shaft in metres
S^e, S^i	Teeth shear surface of the shaft and sleeve in m^2
$t(z)$	Running torque in Nm
T^e_β	Shaft torque of the analytical equation with optimised I^e in Nm
T^e, T^i	Shaft torque at section z in Nm
T^e_{EF}	Shaft torque of the FE model in Nm
T'_{ext}	External torque per unit width in N
T_o	External torque applied to the spline coupling in Nm
$v_{sl}{}^e$, $v_{sl}{}^i$	Shaft and sleeve radial displacement due to sliding in metres

1. Introduction

Involute spline couplings are used as an easy dismountable link between two rotating parts as shown in Fig. 1. In high power transmission, the sizing of spline coupling can be complex and often requests the development of three dimensional finite element models. From the economic point of view, in most everyday industrial applications, the need to dimension systems quickly remains a priority. Several studies [1-5] show that the axial load distribution on the teeth is non-uniform and therefore contradicts standardisation assumptions related to spline coupling sizing [6-8]. This can have harmful consequences. For example, errors in dimensioning can lead to failure despite correct dimensioning in accordance with standards. It is therefore advantageous to be able to develop fast analytical methods allowing for direct analysis of the most significant parameters describing the behaviour of spline coupling, especially avoiding Finite Elements model development.

According to Tatur and Vygonnyi [3], axial torque distribution can be calculated thanks to the equation **(1)**, where the running torque *t(z)* is the torque transmitted from the external spline to the internal spline along the axial direction *z*. *t(z)* is directly linked to the mean pressure acting on section *z*:

$$t(z)=\frac{dT^e(z)}{dz}=c_\varphi\left[\varphi^i(z)-\varphi^e(z)\right], \qquad \textbf{(1)}$$

where $T^e(z)$ is the shaft torque (for every *z*, the sum of $T^e(z)$ and $T^i(z)$, the sleeve torque, being equal to the external torque T_o), c_φ is the torsional stiffness of the joint, considered as constant whatever the value of *z*, and $\varphi^i(z)$ and $\varphi^e(z)$ are the twisting angles for the internal spline and external spline:

$$\frac{d\varphi^i(z)}{dz}=\frac{T^i(z)}{G^iI^i} \text{ and } \frac{d\varphi^e(z)}{dz}=\frac{T^e(z)}{G^eI^e},$$

where G^i and G^e are the shear modulus for the internal spline and external spline, I^i and I^e are the second moment of area for the internal spline and external spline.

Equation **(1)** can be developed to obtain the distribution torque along the shaft or sleeve. Using the expression of the twisting angles, **(1)** gives:

$$\frac{d^2T^e(z)}{dx^2} = c_\varphi\left(\frac{T^e(z)}{G^eI^e} - \frac{T^i(z)}{G^iI^i}\right),$$

A new equation is obtain by replacing $T^i(z) = T_o - T^e(z)$:

$$\frac{d^2T^e(z)}{dx^2} = c_\varphi\left(\frac{T^e(z)}{G^eI^e} - \frac{T_o - T^e(z)}{G^iI^i}\right)$$

After simplification and resolution of this differential equation, the shaft distribution torque is obtained. It expression is gives at the equation **(2)**.

$$T^e(z)=\frac{A}{k}\left(e^{kz}-1\right)-\frac{B}{k}\left(e^{-kz}-1\right), \qquad \textbf{(2)}$$

where:

$k=\sqrt{c_\varphi\left(\frac{1}{G^iI^i}+\frac{1}{G^eI^e}\right)}$, $A=T_o\left(\frac{k+\frac{c_\varphi}{kG^iI^i}\left(e^{-kL}-1\right)}{e^{kL}-e^{-kL}}\right)$, $B=A+\frac{c_\varphi T_o}{kG^iI^i}$, L the spline coupling length.

Equation **(2)** is governed by three parameters: torsional stiffness, shaft, and sleeve second moment of area. The accuracy of the results is highly dependent on the values given to these parameters. It is therefore important to assign the appropriate values to c_φ, I^e and I^i.

A number of studies have been devoted to the evaluation of c_φ. Analytical methods were developed by Hayashi I. and Hayashi T. [9] or Marmol *et al.* [10]. These methods are analysed in a recent work by Barrot *et al.* [11]. However, it appears that they fail to take all phenomena that can be present in such a joint into account. In the study by Barrot *et al.*, an algorithm was proposed to determine the torsional stiffness of involute spline couplings. This

algorithm takes into account the pressure distribution on the teeth flanks, geometric properties and teeth distortion. In the preliminary study in the first stage of the design process, this method turned out to be difficult to apply.

Few articles address the determination of I^e and I^i for spline coupling. Tjenberg [4] and Isakower [12] propose two methods but do not evaluate the consequence of their choice. Second moments of area remain difficult to determine, due to the behaviour of the spline coupling teeth.

The present paper firstly presents how the algorithm developed in Barrot *et al.* [11] is used to construct a simplified method to calculate c_φ.. Secondly, a process to calculate the shaft and sleeve second moment of area is detailed.

2. Torsional stiffness estimation, c_φ

As with teeth gear stiffness determination, studied by example by Cornell [13], the spline geometry requires the shaft and sleeve teeth to be divided up into segments. Moreover, an analytical method, dedicated to determining torsional stiffness of standard involute spline couplings, was developed in a previous work [11]. This method seeks to consider the interdependence between teeth distortions and pressure distribution in its calculations.

In the present paragraph, a simplified and quicker method is proposed. This can be used for involute spline couplings. Torsional teeth stiffness estimation commences by analysing its expression as follows:

$$c_\varphi = \frac{T'_{ext}}{\theta_g}, \qquad \textbf{(3)}$$

where, T'_{ext} is the moment applied on the contact surface per unit width and θ_g is the global rotation. Thanks to the algorithm developed [11], T'_{ext} can be used to determine θ_g. Then, for different T'_{ext} values, a unique c_φ.value is obtained. Thus in the present study, to determine

torsional stiffness the considered value of T'_{ext} is the unit (1N). θ_g represents the sum of various movements due to the superposition of five phenomena identified by Marmol *et al*. and Barrot *et al.*: bending of the teeth, shear of the teeth, compression, tooth foundation rotation and sliding.

$$\theta_g = \theta_b + \theta_s + \theta_c + \theta_f + \theta_{sl},$$

where θ_b is the rotation due to bending of the teeth of both sleeve and shaft, θ_s the rotation due to shear of the teeth of both sleeve and shaft, θ_c the rotation due to compression at the contact, θ_f the rotation due to teeth foundation rotation of the sleeve and the shaft. These rotations depend on a number of factors: contact pressure, teeth geometry, and material. θ_{sl} is the rotation due to sliding between the internal and external spline teeth. This rotation depends on the same factors as the others but to be determined also requires knowledge of the internal and external diameters of the spline coupling. All these rotations are illustrated in Fig. 2. The dependence between rotations and the cited factors precludes describing global rotation using a single equation.

One solution is to consider global rotation as a sum of two entities. The first entity takes into account rotations that do not depend on the inside and outside diameters, while the second takes into account rotation due to sliding. This method can be used if certain basic assumptions are respected, with all sections being straight before and during distortion and only long spline couplings being used.

2.1. Rotations not dependent on inside and outside diameters

According to Barrot *et al.* [11], rotation equations due to bending, shear, compression, and foundation rotation do not depend on the outside and inside diameter of the spline coupling. A simplified analytical equation to determine the sum of these four rotations, known as θ_{ws}, has then to be determined:

$$\theta_{ws} = \theta_b + \theta_s + \theta_c + \theta_f$$

To describe a phenomenon, an equation can be used accounting for a set of parameters. Not all such parameters have the same weight in the final equation and may lead to unnecessary complexity. Identifying the most appropriate parameters is therefore essential in formulating the equation that fits.

- *Search for relevant parameters*

An attempt will now be made to reduce the number of parameters.

The equations describing these rotations depend on the circular pitch, P, the number of spline coupling teeth, N and finally the material parameters G^i and G^e. To facilitate calculation, a modulus m, equal to P/π is applied.

The modulus and number of teeth parameters are linked by the pitch diameter, D. One way of reducing the number of parameters could be to replace m and N by D alone. This would be acceptable if two different involute spline couplings having the same pitch diameter also have identical values for θ_{ws} rotations. A test is conducted for a first spline coupling where N=18, m=2.5mm and a further test where N=27, m=1.667mm leading to a common value for D = 45mm. The gap between the results is 34 per cent, precluding the D alone being considered in the equations.

The material parameters G^i and G^e can also be studied. A solution to reduce the number of parameters could involve introducing the ratio between these two parameters. Thus, a test is conducted with the same spline coupling where the material couple is $G^i/G^e = 1$ with steel-steel and aluminium-aluminium couples. A Gap of θ_{ws} is obtained close to 200 per cent. This result attests to the impossibility of considering only the G^i/G^e ratio to describe the material parameters. According to American standardisation [6, 7] and the most conventional uses of involute spline couplings, this study proposes to establish the law of torsional stiffness

for two material couples: steel-steel and brass-steel (brass for the sleeve). The work presented is available for the commonest modulus and number of teeth.

- *Search for influential parameters*

Various parameters to calculate θ_{ws} were identified. The next step was to highlight the most influential ones. To this purpose, an approach using experimental design was developed. This method is commonly used and is explained through for example in the work by Goupy [14] and by Brisset *et al.* study [15].

This process comprises inputs known as factors and outputs known as responses. The factor values can be continuous or discrete. The plan for a two-level design uses +1 and –1 notation to denote respectively the "high level" and the "low level" for each factor. In searching for the θ_{ws} equation, the proposed factors are *m* and *N*. The levels are defined as:

For the modulus, –1 = 1.25mm and +1 = 2.5mm.

For the number of teeth, –1 = 12 and 1 = 22.

Remark: this study is available for a steel-steel spline coupling.

This process requires four trials to be conducted with each factor set to high or low values as described in the matrix of Tab. 1 in the three first columns. The fourth column, *m N*, corresponds to the interaction between factors on the response, obtained by multiplying *m* level with *N* level for each trial.

Finally, the model for the experiment is:

$$\mathbf{Y} = E\ \mathbf{X},$$

where **Y** is the vector consisting of the four trial responses, E (E_0, E_1, E_2, E_3), the unknown coefficients called factor effects, and **X** the vector consisting of the factors and interaction. E_0 correspond to the average of responses, while E_1, E_2 and E_3 correspond

respectively to the effect of the factors *m* and *N* and the interaction *m N*. For the E_i effect of the i factor, the equation is:

$$E_i = \frac{1}{4}\sum_{j=1}^{4} x_j.y_j$$

with y_j the response of the i factor of j trial, and x_j the level of this factor for the trial.

The experimental design graph is shown in Fig. 3. Each effect of the factors or interaction is represented by a straight line, which can be expressed by the generic equation $y = E_i x + E_0$, with *y* the response, and *x* the level for the factor.

It appears that all factors and interactions give different response values for low and high levels. Thus all parameters can be considered to be influential in the equation for determination of rotation without sliding.

To find the simplified equation for θ_{ws}, its variations according to *m* and *N* must be known. Using analytical results from Barrot's algorithm, the change in θ_{ws} can be determined. Fig. 4 represents this change for a fixed modulus and a fixed number of teeth respectively.

The form of the analytical result of the rotation evolution suggests a polynomial form of the solution. Then θ_{ws} can be:

$$\theta_{ws} = \mathrm{f}(N^3, N^2, N, m^2, m, m\,N).$$

Optimisation using the least squares method to reduce the gap between the analytical values and the sought equation gives the result shown in Fig. 4. A comparison between the analytical and optimised results highlights the difference between them. θ_{ws} must be known with greater accuracy. It is therefore impossible to describe it using the first suggested equation. Another proposition is to establish an equation for each material couple and for each modulus. θ_{ws} form is yet:

$$\theta_{ws} = \mathrm{f}(N^3, N^2, N).$$

A new comparison between the θ_{ws} simplified equation and the analytical result is shown in Fig. 5. This represents a case for m = 1.25mm and the steel-steel material couple. This figure reveals good correlation between the results, and suggests that generalisation to the other modulus can be performed. Finally, equations for the most popular modulus and for two commonest material couples are summarised in Tab.2. The N interval is between 12 and 30. The last column represents the correlation between the analytical result and the proposed equation. Correlation is measured using the Pearson Product Moment Correlation. A correlation of +1 means that there is a perfect positive relationship between results. The good correlation results show that θ_{ws} can be easily calculated by using the equation of Tab. 2.

2.2. Rotation depending on inside and outside diameters

The second part of global rotation is rotation due to sliding [11]. Equations describing sliding depend on inside and outside diameters. The principal equations are recalled below:

$$\theta_{sl} = \frac{2\pi}{P\,N}\left(v_{sl}^{e} + v_{sl}^{i}\right)\tan\left(\phi + \frac{\frac{\pi}{N} + 2\,(\tan(\phi) - \phi)}{4}\right),$$

where:

- ϕ is the contact angle at the pitch radius in radians. A $\frac{\pi}{12}$ (30°) value is commonly used for involute spline coupling deisgn,
- $v_{sl}^{e} = \frac{p_r^{e}\,R_{re}}{\mathrm{E}^{e}\left(R_{re}^{2} - R_{int}^{2}\right)}\left(\left(1-\upsilon\right)R_{re}^{2} + \left(1+\upsilon\right)R_{int}^{2}\right)$,
- $v_{sl}^{i} = \frac{p_r^{i}\,R_{ri}}{\mathrm{E}^{i}\left(R_{ext}^{2} - R_{ri}^{2}\right)}\left(\left(1-\upsilon\right)R_{ri}^{2} + \left(1+\upsilon\right)R_{ext}^{2}\right)$,
- R_{ext} is the external radius of the sleeve, R_{int} is the hole radius of the shaft
- R_{re}, R_{ri} are the foundation radii of the external and internal spline

- The radial component of the contact pressure is uniformly distributed over the outside diameter for the shaft and inside diameter for the sleeve. For the shaft, the resulting equivalent pressure is $p_r^e = \frac{F\ \sin(\phi_p)}{2\sin\left(\frac{\pi}{N}\right) R_{re}}$, and for the sleeve the resulting equivalent pressure is $p_r^i = \frac{F\ \sin(\phi_p)}{2\sin\left(\frac{\pi}{N}\right) R_{ri}}$,

- ϕ_p is the contact load angularity at the pitch radius. The expression of ϕ_p is $\phi_p = \tan\left(\text{asin}\frac{2R_b}{mN}\right) - \frac{\pi}{2N} - \tan(\phi) + \phi$, R_b is the base radius and F the force applied on the contact surface per unit width.

All parameters dependent on geometry or material except the force F, which depends on the tilted angle, α, shown in Fig. 6. To evaluate exactly F, a method, applied in Barrot [11], takes into account the equilibrium law applied to the external spline on the shaft section centre. This equation establishes a link between F, T'_{ext}, R_b, N and the teeth distortion represented by the tilted angle α, as shows equation **(4)**. c represents the half contact length of tooth and χ is Kolosov's constant and μ the modulus of rigidity. Calculation of the tilted angle requires the pressure distribution on teeth flank to be known, imposing an iterative calculus. The difficulty in determining the tilted angle requires a simplified form of F to be established. The suggested equation, where k_F is a corrective coefficient that optimises the rotation due to sliding, is equation **(5)**.

$$F = \left(\frac{T'_{ext}}{N R_b} + \frac{c^2 \pi \alpha}{2 R_b A_K} \right) \text{ where } A_K = \frac{\chi + 1}{4\mu} \qquad \textbf{(4)}$$

$$F = k_F \frac{T'_{ext}}{N R_b} \quad \textbf{(5)}$$

Estimation of the coefficient k_F requires determination of the validity domain. As in the previous paragraph, an experimental design is developed to highlight the different influential factors. The graphic representation is shown in Fig. 7.

The factors taken into account are the ratios for the outside diameter, D_{ext} by the pitch diameter D, the inside diameter, D_{int} by the pitch diameter, the modulus and the number of teeth. Experimental design is conducted for a steel-steel material couple. The levels are:

For D_{ext}/D, –1 = 1.25 and +1 = 2.

For D_{int}/D, –1 = 0 and +1 = 1.2.

For N, –1 = 16 and +1 = 28.

For m, –1 = 1.25mm and +1 = 2.5mm.

Fig. 7 reveals that all factors and interactions have a negligible influence on the corrective coefficient.

Finally, a value of k_F can be found for the various material couples. For the steel-steel couple, $k_F = 0.9879$ and for the brass-steel couple, $k_F = 0.9898$. These coefficients are available for range of N between 12 to 30 for a modulus from 1.25mm to 5mm. This factor increases the accuracy of the value of the θ_{sl} of less than 2 per cent. It can be thus considered that for the presented cases k_F can be removed.

2.3. Torsional stiffness validation

For each modulus, the simplified equations to estimate c_φ are checked. A selection of comparisons between the torsional stiffness obtained by the analytical method from Barrot *et al.* [11] and the simplified equations is shown in Tab. 3. It appeared to be of interest also to compare the simplified equation results with torsional stiffness calculated by the FE model.

The gap between the analytical method and simplified equations for the different tests is less than 5 per cent, being enough to consider that torsional stiffness is known with a good estimation. The developed equations are available for long spline couplings, where the sleeve material can be steel or brass and the shaft material is steel. This model is valid for the considered domain, where *N* can vary between 12 and 30 and *m* between 1.25mm and 5mm.

3. Shaft and sleeve second moment of area determination I^e, I^i

According to the literature, various solutions exist to determine second moments of area of internal and external spline. During this study, various calculations of I^e and I^i are proposed. To determine the most appropriate one, torque distribution along the spline coupling was analysed. This distribution is obtained thanks to the Tatur and Vygonnyi differential equation **(2)** solution and Finite Element model results. The value for torsional stiffness used was obtained by applying the simplified equations presented in the first section of the present article.

3.1. Different calculation possibilities

Four determinations were checked as illustrated in Fig. 8.

- Second moment of area calculated with the part bodies (Fig. 8a)

The ends of the two parts are the outside limits D_{ext} and D_{int} and the teeth are ignored. The other limits are the teeth foundations, D_{re} and D_{ri}. Finally, shaft and sleeve second moments of area equations are respectively:

$$I_b^e = \frac{\pi\left(D_{re}^4 - D_{\text{int}}^4\right)}{32} \text{ and } I_b^i = \frac{\pi\left(D_{ext}^4 - D_{ri}^4\right)}{32}. \quad \textbf{(6)}$$

This Tjenberg [4] method is used to apply equation **(1)**. In Isakower [12], the final second moments of area are obtained with an increase in 10 per cent in this value.

- Second moments of area calculated with the teeth end diameters (Fig. 8b)

As previously, external limits are identical, and the other diameters are the major diameters. Shaft and sleeve second moment of area equations are respectively:

$$I_t^e = \frac{\pi\left(D_0^4 - D_{\text{int}}{}^4\right)}{32} \text{ and } I_t^i = \frac{\pi\left(D_{ext}^4 - D_i^4\right)}{32}. \quad \textbf{(7)}$$

- Second moments of area are calculated with the pitch diameter (Fig. 8c)

When influence of the teeth is taken into account with the pitch diameter the equations for shaft and sleeve second moments of area are respectively:

$$I_p^e = \frac{\pi\left(D^4 - D_{\text{int}}^4\right)}{32} \text{and } I_p^i = \frac{\pi\left(D_{ext}^4 - D^4\right)}{32} \quad \textbf{(8)}$$

- Second moments of area calculated with influence of teeth shearing (Fig. 8d)

Second moments of area can be divided into two parts: the body and the teeth. The second moment of area of the two parts is the sum of the individual second moments of area.

For the external spline, the second moment of area of the body is calculated at the centre of the spline section: $I_{body}^e = \frac{\pi\left(D_{re}^4 - D_{\text{int}}^4\right)}{32}$. The shaft tooth second moment of area, at the tooth's centre of gravity is negligible. This moment, at the centre of the shaft section can be determined from the Huygens theorem: $I_{tooth}^e = \frac{S^e D^2}{4}$, where S^e is the shaft shear surface in a section plane. Finally, for a spline coupling the equations are:

$$I_s^e = \frac{\pi\left(D_{re}^4 - D_{\text{int}}^4\right)}{32} + \frac{S^e N D^2}{4} \text{ and } I_s^i = \frac{\pi\left(D_{ext}^4 - D_i^4\right)}{32} + \frac{S^i N D^2}{4}, \quad \textbf{(9)}$$

where S^i is the sleeve shear surface in a section plane.

3.2. Method for determination of spline coupling second moments of area

In order to select the best method of second moment of area evaluation, a reference has to be chosen. The 3D FE method is used for this. Indeed, various research works as with

Barrot *et al.*, Leen *et al.*, Limmer *et al.*, Sum *et al.*, [2, 16-19] have shown that FE simulation and experimental studies give similar results.

Three dimensional finite element models using ABAQUS have been developed for different spline couplings. The meshing used to model the two parts making up the coupling, the shaft and sleeve are shown in Fig. 9 and is composed by 26000 solid linear brick elements and 30000 nodes. The boundary conditions are defined as follows. The contact is specified on the teeth flanks (with no friction). This condition imposes a non linear resolution. The nodes of a sleeve's extremity are locked but radial expansion is allowed, as the figure illustrates with the small arrows. Nodes of the opposite shaft end can't move in the axial direction and a torque is applied to the same shaft surface. The loading is introduced by forces on nodes of the shaft surface, in order to introduce a linear shear stress on the section. Cyclic symmetry conditions are used on the two lateral surfaces to simulate behaviour of the complete spline coupling.

Comparison is made between the axial torque distribution according to FE models and the analytical model with different second moments of area calculation. The test is performed for four different involute spline couplings as described in Tab. 4 and the results are shown in Fig. 10. The torque transfer between the internal and external spline is located in particular at the ends of spline coupling. Indeed, it has been established for the load configuration shown in Fig. 9 that the pressure peaks are at the extremities [2, 4, 5]. If the gap between torque distribution result of FE and analytic models decreases, accuracy of knowledge on maximum pressure will be enhanced.

In accordance with the results shown in Fig. 10, the best calculation is that which takes shear teeth influence into account.

In calculation of the second moments of area, the error computed can be due to the influence of the teeth. This influence is less significant for the sleeve second moment of area

than for the shaft. This explains why it is necessary to determine whether an optimisation of the shaft second moment of area can increase accuracy of the torque distribution result. In the next study, the new second moments of area considered are $I^i = I^i_s$ and $I^e = \beta I^e_s$.

Moreover, thanks to this optimisation, and if the influence of the external diameter of the spline coupling is taken into account, the errors in the basic hypotheses of equation **(1)** can also diminish the end-contact effect, which can be neglected.

An experimental design is developed to estimate the influence of N, m and D_{ext}/D on a population of spline couplings. For every spline couplings, the ratio D_{ext}/D allows the same skin thickness above the sleeve teeth to be checked. An experimental design with 3 factors and 2 levels, corresponding to 9 tests, is conducted. The different levels are as follows:

For N –1 = 14 and +1 = 30

For m –1 = 1.25mm and +1 = 5mm

For D_{ext}/D –1=1.25 and +1=2

The responses β_0 are obtained with minimisation of the gap between analytical and FE torque distribution using the least squares method.

Fig. 11 stresses the influence of factors and interactions taken into account in the experimental design. This graph shows that only the interaction of a high order appears not to be influential, i.e. having a value that has little effect on the response.

To determine the equation for the corrective coefficient β, a linear form is proposed. This is a function of the previous factors and interactions. To find the effect values of these parameters, the least squares method is used. It is important to note that to increase the precision of the β equation, 27 tests are performed. In fact a new level is added: N = 22, m = 2.5mm, D_{ext}/D = 1.625.

The following equation is found:

$$\beta = 6.958\times10^{-2}\,m + 2.742\times10^{-2}\,N + 2.937\times10^{-1}\,\frac{D_{ext}}{D} \\ -3.396\times10^{-3}\,m\,N + 2.036\times10^{-2}\,m\frac{D_{ext}}{D} - 3.86\times10^{-3}\,N\frac{D_{ext}}{D} \quad \textbf{(10)}$$

To estimate the accuracy of **(10)**, a comparison between β and β_0 is highlighted in Tab. 5, which presents the gap, Gap_β in per cent, corresponding to:

$$Gap_\beta = 100\frac{\beta - \beta_0}{\beta_0}$$

The average result is about 6%.

To evaluate the influence of the corrective coefficient, a calculation of the σ ratio between the model before and after correction is made. σ values are shown in the last column. This ratio is the division of the sum of the least squares fit between the analytical equation and FE model results and sum of the least squares fit between the analytical equation and FE model results.

$$\sigma = \frac{\sum\left(T^e - T^e_{FE}\right)^2}{\sum\left(T^e_\beta - T^e_{FE}\right)^2} \quad \textbf{(11)}$$

Where, T^e is the shaft torque value of the analytical equation, T^e_{FE} is the torque value of the FE model and T^e_β is the torque value of the analytical equation, with the optimised shaft second moment of area.

The ratio represents the gain due to β. Tab. 5 reveals that β allows the accuracy of almost all torque distributions to be improved by a factor of two on average.

3.3. Second moment of area calculation validation

The utility of the corrective coefficient on the shaft second moment of area determination was highlighted in the previous paragraph. It is important to validate equation **(10)** on other spline couplings that are not used to determine this equation. Tests are conducted for four involute spline couplings, described in Tab. 6. It is possible to calculate the

gap between the FE results and the analytical results with and without β. Taking the FE as reference, Fig. 12 illustrates these gaps along *z*-axis. According to Tab. 6 and Fig. 12, introducing β to calculate I^e increases torque distribution accuracy on all the studied spline couplings.

4. Conclusion

Thanks to Tatur, there is an equation to estimate torque distribution along the spline coupling. This equation requires knowledge of torsional stiffness and shaft and sleeve second moments of area. In a previous study, a complex algorithm to determine the torsional stiffness of involute spline couplings was performed. In this paper simplified equations are proposed that are easily and rapidly used.

To determine the most appropriate equations, experimental designs are analysed.

Torsional stiffness is the result of rotations due to various distortion phenomena such as bending, shear, compression, rotation of teeth foundation and sliding of the teeth. These rotations are divided into two parts. The first takes into account the four first phenomena and the second addresses the issue of sliding. Two simplified equations are finally expressed to define stiffness. In this study two couples of materials are considered: steel – steel and brass – steel. The influential factors are highlighted through various experimental designs, and the equations are developed using the least squares method. A comparison with the simplified method and the complex algorithm underlines the good estimation of torsional stiffness.

This paper analyses several analytical solutions to describe these parameters, and reveals that the second moments of area have considerable influence on distribution. One particular solution that takes the teeth shear into account, is proposed as being the most effective. To increase accuracy, a β coefficient was added and its analytical detailed. The said coefficient is capable of enhancing accuracy of torque distribution analysis three-fold.

References

[1] **Adey, R. A., Baynham, J. and Taylor, J. W.** Development of analysis tools for spline couplings. *Institution of Mechanical Engineers, Part G: Journal of Aerospace Engineering*, 2000, **214**(6)**,** 347-357.

[2] **Barrot, A., Paredes M., Sartor, M.** An assistance tool for spline coupling design, *Recent Advances in Integrated Design and Manufacturing in Mechanical Engineering*, edited by Bramley, A., Eds. Dordrecht, Springer, ISBN 1402034814, Springer, 2005, 329-342.

[3] **Tatur, G. K. and Vygonnyi, A. G.** Stress Sources and Critical Stress Combinations for Splined Shaft. *ASME, Journal of mechanical design*, 1969, **XLIX**(4)**,** 23-29.

[4] **Tjernberg, A.** Load distribution in the axial direction in a spline coupling. *Engineering Failure Analysis*, 2001, **8**(6), 557-570.

[5] **Volfson, B. P.** Stress sources and critical stress combinations for splined shaft. *Journal of Mechanical Design*, 1982, **104**(3), 551-556.

[6] **American standardization**. Spline coupling (in metric) ANSI B92.2M-1980 (R 1989), 1989.

[7] **American standardization**. Spline coupling (in inch) ANSI B92.1-1970 (R 1993), 1993.

[8] **French standardization**. Cannelures cylindriques droites à flancs en développante et centrage sur flancs – Angles de pression 30°, 37,5° et 45°, NF E-22 144, 1987.

[9] **Hayashi, I. and Hayashi, T.** Miniaturisation of involute splined couplings. Discussion from torsional stiffness and yield torque. *Bulletin of the JSME*, 1985, **28**(236), 259-266.

[10] **Marmol, R. A., Smalley, A. J. and Tecza, J. A.** Spline coupling induced nonsynchronous rotor vibrations. *ASME, Journal of mechanical design*, 1980, **102**(1)**,** 168-176.

[11] **Barrot, A., Paredes M., Sartor, M.** Determining both radial pressure distribution and torsional teeth stiffness of involute spline coupling. *Institution of Mechanical Engineer. Part C: Journal of mechanical engineering science*, 2006, ISSN:0954-4062, **220(**12), 1727-1738.

[12] **Isakower, R. I..** Don't guess on non-circular shafts. *Design Engineering*, November 1980.

[13] **Cornell, R. W.** Compliance and stress sensitivity of spur gear teeth. *ASME, Journal of mechanical design*, 1981, **103**(2)**,** 447-459.

[14] **Goupy, J.** Introduction aux plans d'expériences. *Technique et ingénierie, Série conception*, 2001, edited by Dunod, ISBN: 2100056069.

[15] **Brisset, S., Gillon, F. Vivier, S. and Borchet, P.** Optimization with experimental design. An approach using Taguchi's Methodology and Finite Element simulations. *Transactions on Magnetics*, 2001, **37**(5).

[16] **Leen, S. B., Hyde, T. R., Williams, E. J., Becker, A. A., McColl, I. R., Hyde, T. H. and Taylor, J. W.** Development of a representative test specimen for frictional contact in spline joint couplings. *Journal of Strain Analysis for Engineering Design*, 2000, **35**(6), 521-544.

[17] **Leen, S. B., Richardson, I. J., McColl, I. R., Williams, E. J. and Hyde, T. R.** Macroscopic fretting variables in a splined coupling under combined torque and axial load. *Journal of Strain Analysis for Engineering Design*, 2001, **36**(5), 481-497.

[18] **Limmer, L., Nowell, D. and Hills, D.** A. A combined testing and modelling approach to the prediction of the fretting fatigue performance of splined shafts. *Institution of Mechanical Engineers, Part G.: Journal of Aerospace Engineering*, 2001, **215**, 105-111.

[19] **Sum, W. S., Williams, E. J. and Leen, S. B.** Finite element, critical-plane, fatigue life prediction of simple and complex contact configurations. *International Journal of Fatigue*, 2005, ISSN: 0142-1, 123 **27**(4), 403-416.

Tables

Number of the experiment	m	N	$m\,N$	θ_{ws} [rad]
Trial 1	-1	-1	+1	2.03×10^{-5}
Trial 2	+1	-1	-1	5.08×10^{-6}
Trial 3	-1	+1	-1	5.80×10^{-6}
Trial 4	+1	+1	+1	1.46×10^{-6}

Tab. 1 Analysis matrix for the rotation without sliding rotation

Modulus	Material Sleeve	Material Shaft	Equations	R^2
1.25	Steel	Steel	$\theta_{ws} = -5.963\times10^{-9}N^3 + 4.468\times10^{-7}N^2 - 1.229\times10^{-5}N + 1.101\times10^{-4}$	0.99
	Brass	Steel	$\theta_{ws} = -8.424\times10^{-9}N^3 + 6.621\times10^{-7}N^2 - 1.743\times10^{-5}N + 1.566\times10^{-4}$	0.99
1.667	Steel	Steel	$\theta_{ws} = -4.095\times10^{-9}N^3 + 3.070\times10^{-7}N^2 - 7.723\times10^{-6}N + 6.657\times10^{-5}$	0.99
	Brass	Steel	$\theta_{ws} = -5.441\times10^{-9}N^3 + 4.093\times10^{-7}N^2 - 1.039\times10^{-5}N + 9.085\times10^{-5}$	0.99
2.5	Steel	Steel	$\theta_{ws} = -1.825\times10^{-9}N^3 + 1.362\times10^{-7}N^2 - 3.417\times10^{-6}N + 2.944\times10^{-4}$	0.99
	Brass	Steel	$\theta_{ws} = -2.265\times10^{-9}N^3 + 1.738\times10^{-7}N^2 - 4.482\times10^{-6}N + 3.966\times10^{-5}$	0.99
5	Steel	Steel	$\theta_{ws} = -2.314\times10^{-10}N^3 + 1.862\times10^{-8}N^2 - 5.105\times10^{-7}N + 4.875\times10^{-6}$	0.99
	Brass	Steel	$\theta_{ws} = -3.318\times10^{-10}N^3 + 2.674\times10^{-8}N^2 - 7.343\times10^{-7}N + 7.025\times10^{-6}$	0.99

Tab. 2 Equations of rotation without sliding for each couple (modulus, materials)

Modulus [mm]	1.25	1.667	2.5	5
Number of teeth	20	25	24	30
Outside diameter [mm]	37.5	60	90	250
Materiel Couple	Steel-steel	Brass-steel	Steel-steel	Brass-steel
Torsional stiffness obtained by the analytical method from Barrot[9] $\times10^6$ [N/rad]	90.1	150	561	2590
Torsional stiffness obtained by the FE method $\times10^6$ [N/rad]	87.6	152	552	2555
Torsional stiffness obtained by the simplified equations $\times10^6$ [N/rad]	94.0	153	542	2550
Gap between FE model and simplified equations [%]	+7.3	+0.65	-1.81	-0.19
Gap between analytical method and simplified equations [%]	+4.30	1.85	-3.43	-1.49

Tab. 3 Comparison of torsional stiffness for different spline couplings between the complete and simplified methods

Designations	Modulus m	Number of teeth N	Outside diameter D_{ext}	Inside diameter D_{int}
A	1.25	22	34.4	10
B	1.66	27	55	30
C	2.5	18	70	15
D	5	30	188	20

Tab. 4 Spline coupling designation for second moment of area calculus research

m [mm]	N	D_{ext}/D	β_0	β	Gap_β [%]	σ
1.25	14	1.25	0.89	0.76	14.33	1.95
1.25	14	1.625	0.82	0.86	4.60	9.91
1.25	14	2	0.88	0.96	8.70	2.84
1.25	22	1.625	0.98	1.00	1.88	1.01
1.25	22	2	1.11	1.08	2.02	1.99
1.25	22	1.25	1.03	0.91	11.39	1.36
1.25	30	2	1.15	1.21	4.78	1.80
1.25	30	1.25	0.97	1.06	8.82	1.13
1.25	30	1.625	1.01	1.13	11.59	1.01
2.5	14	1.25	0.91	0.82	9.31	1.99
2.5	14	1.625	0.85	0.92	9.11	5.69
2.5	14	2	0.92	1.03	11.88	1.77
2.5	22	2	1.09	1.12	2.41	1.10
2.5	22	1.25	0.96	0.94	1.99	1.40
2.5	22	1.625	0.97	1.03	6.16	1.42
2.5	30	1.25	0.99	1.05	6.70	1.05
2.5	30	1.625	1.10	1.13	3.35	1.38
2.5	30	2	1.33	1.21	9.16	2.35
5	14	1.25	0.94	0.94	0.86	4.60
5	14	1.625	0.99	1.05	5.75	1.00
5	14	2	1.18	1.16	1.98	2.52
5	22	1.25	0.96	1.00	3.44	1.26
5	22	1.625	1.07	1.09	2.49	1.19
5	22	2	1.27	1.19	6.20	3.27
5	30	1.25	0.99	1.05	5.88	1.02
5	30	1.625	1.06	1.13	6.78	1.18
5	30	2	1.26	1.22	3.42	3.00

Tab. 5 Gap between the optimised and calculated corrective coefficient and the influence of this coefficient on torque distribution

Spline coupling	m [mm]	N	D_{ext}/D	I^e_s [mm^4]	β	I^e [mm^4]	σ
A	1.25	18	1.56	2.40×10^4	0.923	2.14×10^4	3.57
B	1.667	20	1.49	1.19×10^5	0.927	1.11×10^5	3.45
C	1.667	27	1.22	3.20×10^5	0.998	3.19×10^5	2.17
D	5	18	1.66	63.3×10^5	1.08	68.3×10^5	1.12

Tab. 6 Second moment of area calculation validation for four different spline couplings

Figures

Fig. 12 Comparison of gap between FE torque distribution and analytical torque distributions for four spline couplings

Author’s name: Barrot

Figure number 1

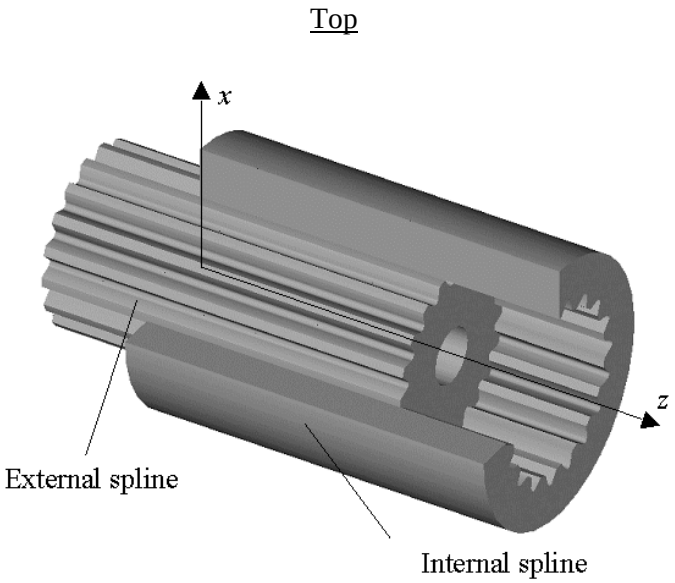

Author's name: Barrot

Figure number 2

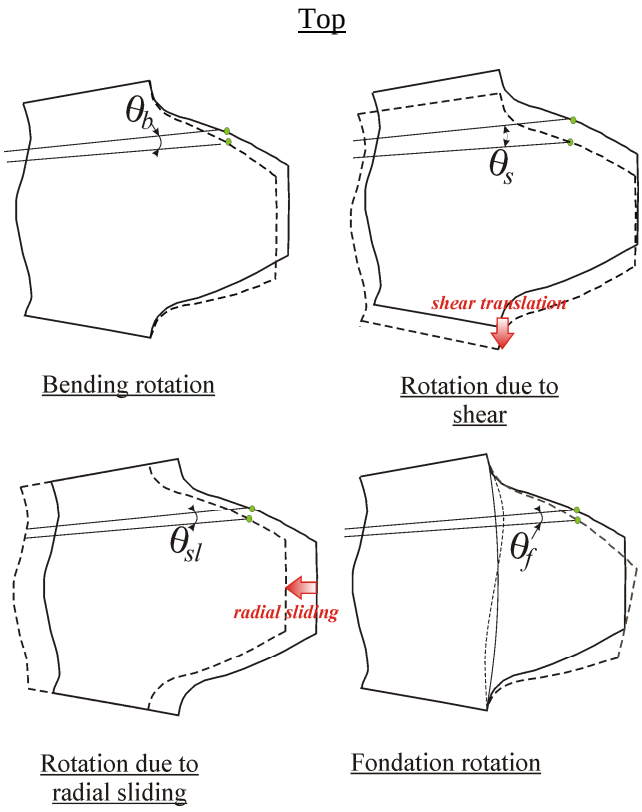

Author's name: Barrot

Figure number 3

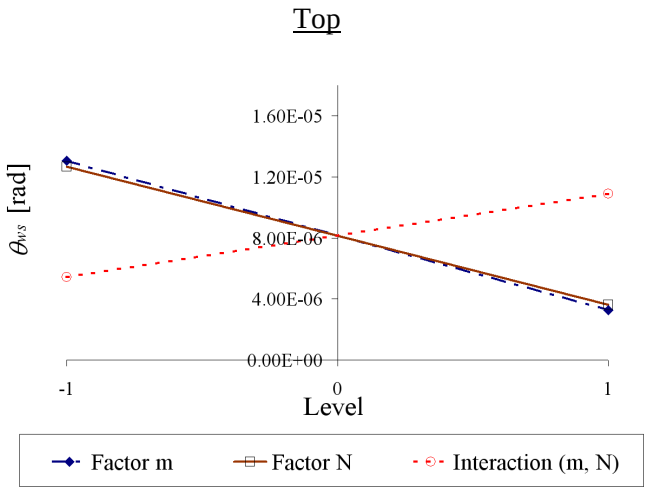

Author's name: Barrot

Figure number 4

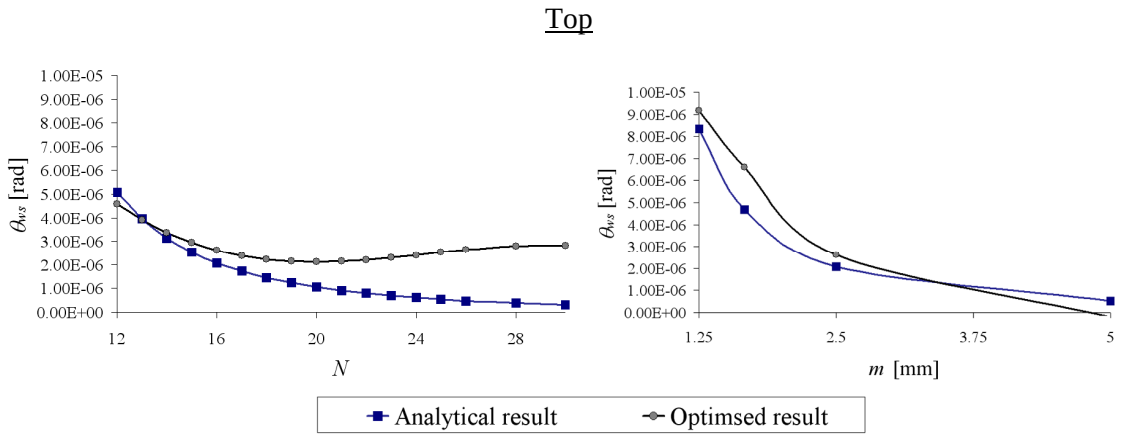

Author’s name: Barrot

Figure number 5

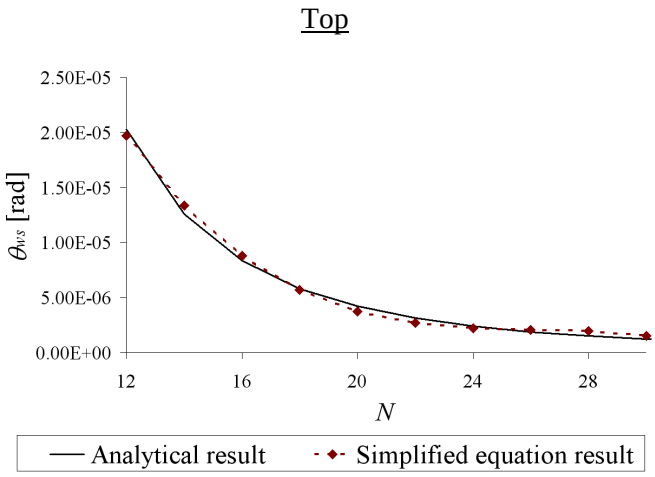

Author's name: Barrot

Figure number 6

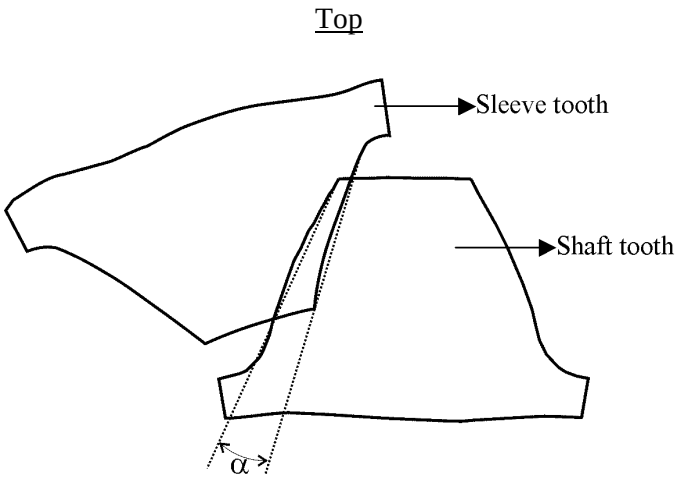

Author's name: Barrot

Figure number 7

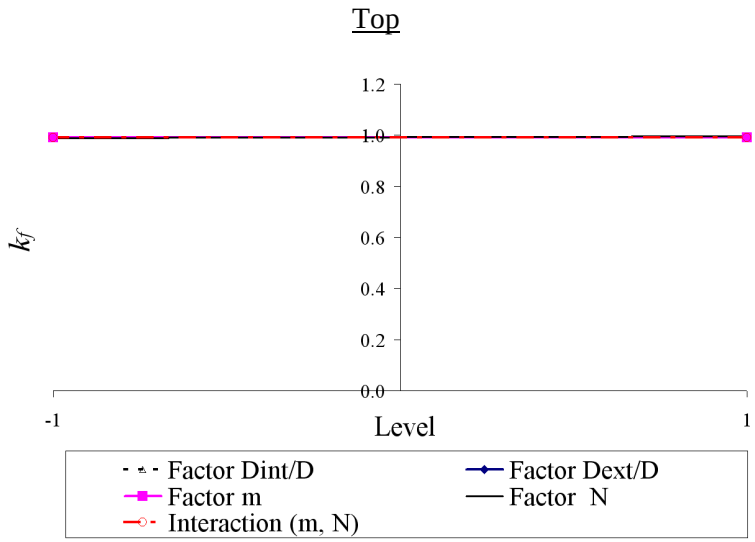

Author’s name: Barrot

Figure number 8

Top

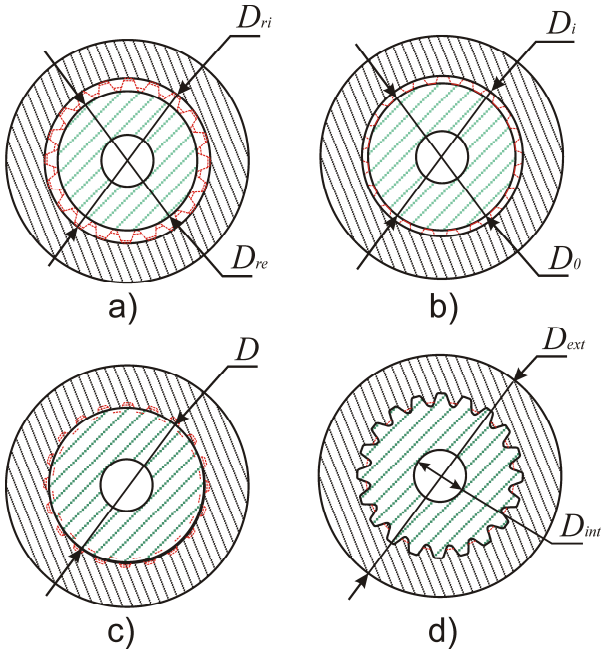

Author’s name: Barrot

Figure number 9

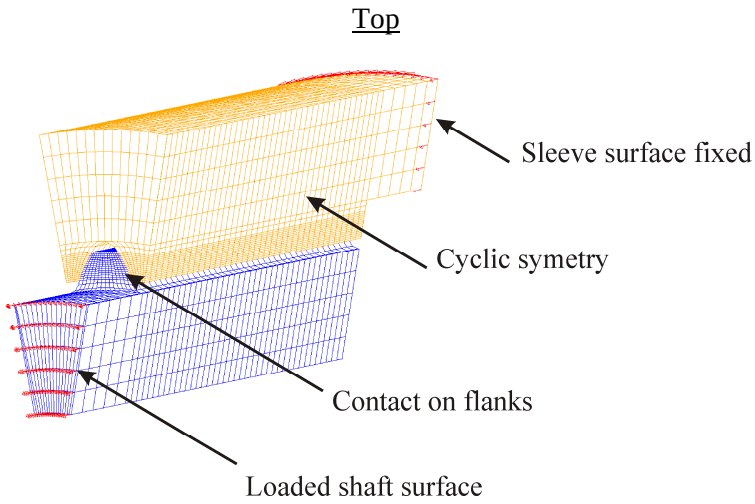

Author's name: Barrot

Figure number 10

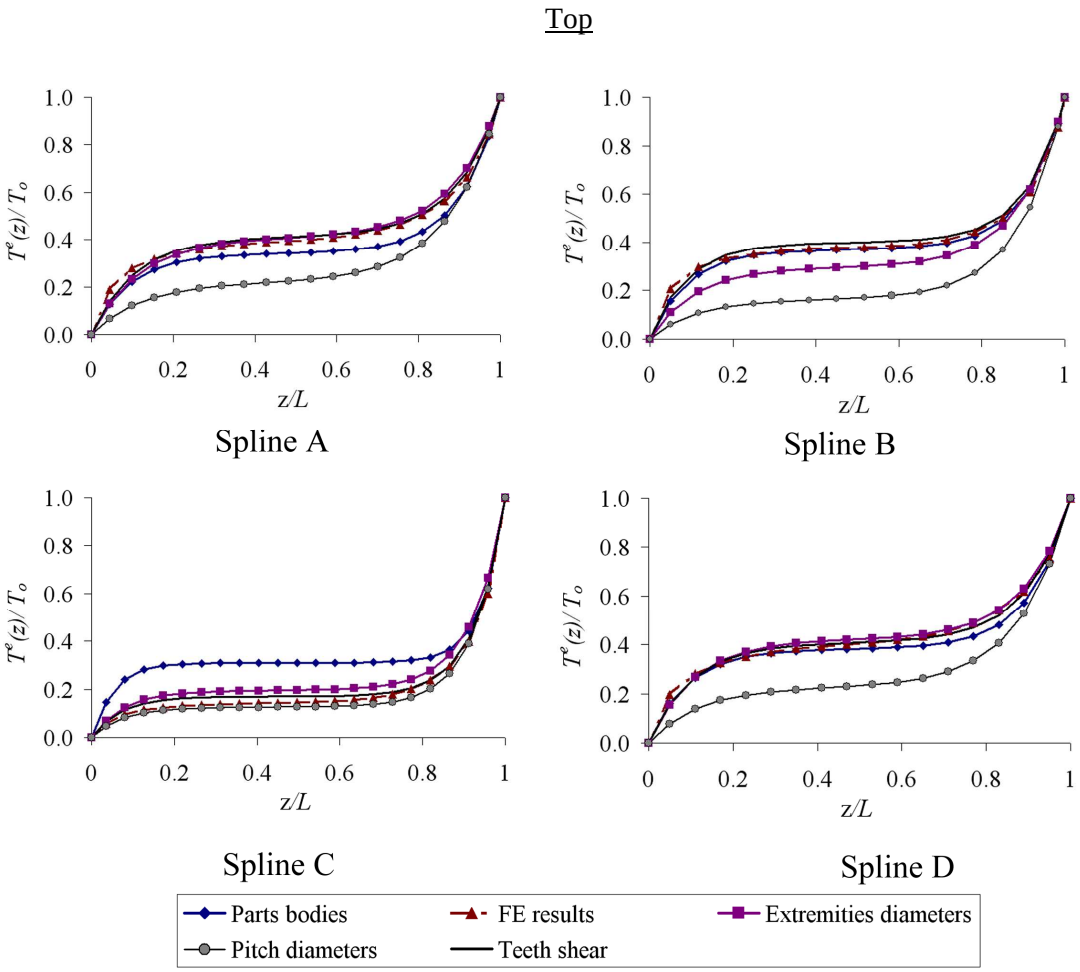

Author's name: Barrot

Figure number 11

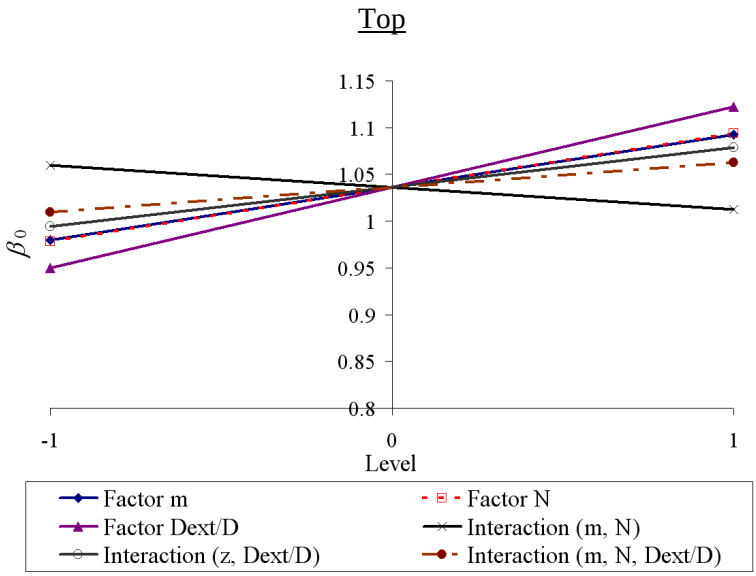

Author's name: Barrot

Figure number 12

Top